RESEARCH ARTICLE SUMMARY

NEURODEVELOPMENT

Human TKTL1 implies greater neurogenesis in frontal neocortex of modern humans than Neanderthals

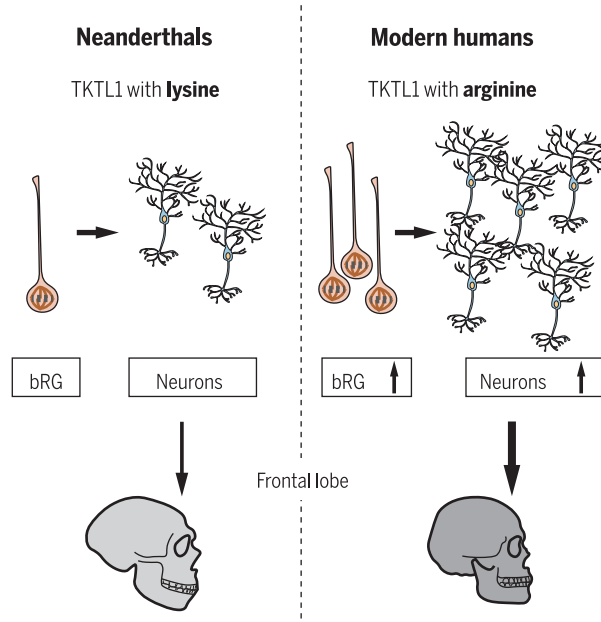Anneline Pinson, Lei Xing†, Takashi Namba†, Nereo Kalebic†, Jula Peters, Christina Eugster Oegema, Sofia Traikov, Katrin Reppe, Stephan Riesenberg, Tomislav Maricic, Razvan Derihaci, Pauline Wimberger, Svante Pääbo, Wieland B. Huttner*

INTRODUCTION: The evolutionary expansion of the neocortex and the concomitant increase in neuron production are considered to be a basis for the increase in cognitive abilities that occurred during human evolution. Endocast analyses reveal that the endocranial volume of modern humans and Neanderthals was similar, suggesting similar brain and neocortex size. But whether similar neocortex size implies similar neocortical neuron production remains unclear.

RATIONALE: *Transketolase-like 1* (*TKTL1*) is a gene from the transketolase family that in fetal human neocortex is preferentially expressed in the two classes of neuroprogenitors, the apical progenitors in the ventricular zone and the basal progenitors in the subventricular zone. The latter class of neuroprogenitors comprises two major types, the basal intermediate progenitors (bIPs) and the basal radial glia (bRG, also called outer radial glia). bRG exhibit cellular processes that promote their ability to self-amplify, and are the neuroprogenitor type considered to be a driver of the increase in cortical neuron production, which is a hallmark of the evolution of the human neocortex. Reflecting their cell polarity, bRG undergo repeated asymmetric divisions that self-renew the bRG and generate one neuron each. Thereby, bRG generate more neurons over time than the other type of neuron-generating basal neuroprogenitors, the process-lacking bIPs whose neurogenic divisions are symmetric self-consuming. TKTL1 is one of the few proteins with a single amino acid substitution found in essentially all present-day humans but absent from extinct archaic humans, the Neanderthals and Denisovans, and other primates. This human-specific amino acid substitution in TKTL1 is a lysine in apes and archaic humans but an arginine in modern humans. We therefore investigated (i) whether TKTL1 has a role in neocortex development and affects neuroprogenitor numbers and (ii) whether both archaic TKTL1 (aTKTL1) and modern human TKTL1 (hTKTL1) exert similar effects on neuroprogenitors during neocortex development.

RESULTS: When expressed in mouse embryo neocortex, which lacks *TKTL1* expression, hTKTL1 increased the abundance of bRG without affecting that of bIPs and that of apical progenitors. The effect of TKTL1 on bRG abundance was limited to hTKTL1; aTKTL1, which differs only by one amino acid, was unable to increase bRG abundance. The greater bRG abundance upon hTKTL1 expression resulted in an increase in cortical neuron production over time, specifically of the late-born upper-layer neurons rather than of the early-born deep-layer neurons. In the folded (gyrencephalic) developing ferret neocortex, *hTKTL1* expression increased not only bRG abundance but also the proportion of bRG with multiple processes, a hallmark of bRG that can self-amplify. As a consequence of this effect, gyrus size increased.

In fetal human neocortex, hTKTL1 was essential to maintain the full number of bRG, as CRISPR-Cas9–mediated hTKTL1 knockout in fetal human neocortical tissue reduced this number. To further demonstrate the relevance of this effect, we converted hTKTL1 to the Neanderthal variant aTKTL1 in human embryonic stem cells and generated minibrain structures called cerebral organoids. The aTKTL1-expressing organoids contained fewer bRG and neurons, hence the human-specific lysine-to-arginine substitution in hTKTL1 is essential for maintaining the full number of bRG and neurons in this human brain model. In fetal human neocortex, hTKTL1 expression in neuroprogenitors increased during the course of neurogenesis and was particularly high in the developing frontal lobe as compared to the developing occipital lobe.

As to its mechanism of action, hTKTL1 increased bRG abundance via two metabolic pathways, the pentose phosphate pathway (PPP) followed by fatty acid synthesis. Inhibition of the PPP or of fatty acid synthesis, using a variety of specific inhibitors, completely suppressed the hTKTL1-induced increase in bRG abundance in embryonic mouse neocortex and reduced bRG numbers in fetal human neocortical tissue. This metabolic action of hTKTL1, but not aTKTL1, in bRG resulted in an increase in the concentration of acetyl–coenzyme A, the critical metabolite for fatty acid synthesis. Our data suggest that hTKTL1, but not aTKTL1, promotes the synthesis of membrane lipids containing a certain type of fatty acid that are required for the outgrowth of bRG processes and hence for the increase in bRG abundance.

CONCLUSION: In light of our finding that *TKTL1* expression in fetal human neocortex is particularly high in the developing frontal lobe, our study implies that because of the single amino acid–based activity of hTKTL1, neocortical neurogenesis in modern humans was and is greater than it was in Neanderthals, in particular in the frontal lobe. ∎

TKTL1 and hominin cortical neurogenesis. The single lysine-to-arginine substitution in modern human TKTL1 leads to greater bRG numbers than in Neanderthals. These bRG in turn generate more neocortical neurons in modern humans. Because TKTL1 expression in fetal human neocortex is particularly high in the developing frontal lobe, these findings imply that the frontal lobe of modern humans contains more neurons than that of Neanderthals.

READ THE FULL ARTICLE AT
https://doi.org/10.1126/science.abl6422

RESEARCH ARTICLE

NEURODEVELOPMENT

Human TKTL1 implies greater neurogenesis in frontal neocortex of modern humans than Neanderthals

Anneline Pinson[1], Lei Xing[1]†, Takashi Namba[1]†‡, Nereo Kalebic[1]†§, Jula Peters[1], Christina Eugster Oegema[1], Sofia Traikov[1], Katrin Reppe[1], Stephan Riesenberg[2], Tomislav Maricic[2], Razvan Derihaci[3], Pauline Wimberger[3], Svante Pääbo[2], Wieland B. Huttner[1]*

Neanderthal brains were similar in size to those of modern humans. We sought to investigate potential differences in neurogenesis during neocortex development. Modern human transketolase-like 1 (TKTL1) differs from Neanderthal TKTL1 by a lysine-to-arginine amino acid substitution. Using overexpression in developing mouse and ferret neocortex, knockout in fetal human neocortical tissue, and genome-edited cerebral organoids, we found that the modern human variant, hTKTL1, but not the Neanderthal variant, increases the abundance of basal radial glia (bRG) but not that of intermediate progenitors (bIPs). bRG generate more neocortical neurons than bIPs. The hTKTL1 effect requires the pentose phosphate pathway and fatty acid synthesis. Inhibition of these metabolic pathways reduces bRG abundance in fetal human neocortical tissue. Our data suggest that neocortical neurogenesis in modern humans differs from that in Neanderthals.

Whether and how cognitive abilities of modern humans might differ from those of extinct archaic humans such as Neanderthals remains a matter of debate (*1*). Discovery of artifacts and art of presumably Neanderthal derivation (*2*, *3*) fuels the debate. Cognitive abilities reside primarily in the neocortex, the largest and most recently evolved part of the brain, which is present only in mammals. The evolutionary expansion of the neocortex and the concomitant increase in neuron production are considered to be a basis for the increase in cognitive abilities that occurred during human evolution (*4*). Analyses of endocasts indicate that the endocranial volume of modern humans and Neanderthals was similar, suggesting similar brain and neocortex size (*5*). But whether similar neocortex size implies similar neocortical neuron production has remained unclear.

One approach to address this question would be to compare key features of neocortex development between modern humans and Neanderthals, using appropriate model systems and focusing on the actions of modern human versus Neanderthal variants of key genes that govern neocortex development. Of particular interest here are genes that influence the behavior of neural progenitor cells (neuroprogenitors) in the fetal neocortex, as their abundance and proliferative capacity determine the number of cortical neurons generated during development (*6*, *7*).

Two principal classes of neuroprogenitors are present in the developing neocortex, referred to as apical progenitors (APs) and basal progenitors (BPs). APs, the primary class, reside in the ventricular zone (VZ). After the onset of neurogenesis, the major AP type is the apical (or ventricular) radial glia (aRG). Rather than producing neurons, aRG generate mostly BPs, the secondary class of neuroprogenitors. Newborn BPs migrate to the subventricular zone (SVZ), from where they generate most of the cortical neurons (*7*).

Two types of BPs have been characterized, referred to as basal intermediate progenitors (bIPs) and basal (or outer) radial glia (bRG). In mammals with a small and lissencephalic neocortex, such as mice, ~90% of the BPs are neurogenic bIPs that typically divide once to give rise to two neurons [(*7*) and references therein]. bRG constitute only ~10% of the BPs in embryonic mouse neocortex (*8*–*10*). In contrast, in ferrets (a gyrencephalic carnivore) and in primates such as marmosets, macaques, and humans, bRG constitute ~50% of the BP pool (*8*, *11*–*13*). This increase in the relative abundance of bRG is considered to drive the increase in cortical neuron production that is a hallmark of the evolution of the human neocortex (*6*, *14*, *15*).

In contrast to bIPs, neurogenic divisions of bRG are typically asymmetric, generating a bRG (self-renewal) and a neuron (*7*, *12*, *13*). This mode of cell division reflects the presence of cell polarity of bRG, evident as a basal process, which is lacking in bIPs (*7*, *12*, *13*). bRG generate more cortical neurons over time than bIPs (*12*).

A gene that could influence the behavior of neuroprogenitors in fetal human neocortex is *transketolase-like 1* (*TKTL1*) (*16*). TKTL1 belongs to the transketolase family of enzymes. It operates in the pentose phosphate pathway (PPP), a metabolic pathway linked to glycolysis (*17*–*19*). We focused on *TKTL1* because: (i) *TKTL1* is preferentially expressed in neuroprogenitors, including bRG, of fetal human neocortex (*20*–*23*). (ii) *TKTL1*, implicated in human tumors (*24*, *25*) and tumor cell proliferation (*19*, *26*), may also increase neuroprogenitor numbers. (iii) TKTL1 is one of the few proteins with an amino acid substitution found in essentially all present-day humans and absent from extinct archaic humans, Neanderthals and Denisovans, and other primates (*27*).

The human-specific amino acid substitution at residue 317 in the long isoform of TKTL1 (corresponding to amino acid residue 261 in the short isoform) is a lysine in apes and archaic humans but an arginine in modern humans (*27*). We therefore investigated (i) whether TKTL1 has a role in neocortex development and affects neuroprogenitor behavior and (ii) whether both archaic TKTL1 (aTKTL1) and modern human TKTL1 (hTKTL1) exert similar effects on neuroprogenitors during neocortex development. We find that hTKTL1 but not aTKTL1 increases the abundance of bRG, but not bIPs, in developing neocortex. We suggest that more neocortical neurons are generated during neurogenesis in modern humans than in Neanderthals.

TKTL1 expression in fetal human neocortex

Analysis of published transcriptome datasets (*21*–*23*) revealed that in the human neocortex at 13 to 16 postconception weeks (PCW), *TKTL1* mRNA is expressed in the VZ and inner and outer SVZ (iSVZ and oSVZ) but not the cortical plate (CP) (fig. S1A). Accordingly, *TKTL1* mRNA is expressed in aRG and bRG isolated from PCW 13 or PCW 16–17 human neocortex. *Tktl1* mRNA is not expressed in embryonic day 14.5 (E14.5) mouse neocortex (fig. S1A). Further analysis showed that the *TKTL1* isoform expressed in fetal human neocortex is the short isoform, encoding a 540–amino acid protein (fig. S1, B, D, and E), with the amino acid change at position 261 (fig. S1H).

Highest *TKTL1* expression in frontal lobe

TKTL1 expression in fetal human neocortex by reverse transcription quantitative polymerase chain reaction was found to increase with development (PCW 9 to 15; fig. S1, D and E). Consistent with a previous report (*28*), *TKTL1* expression increased at PCW 17 in the frontal lobe, but not the occipital lobe, of fetal human neocortex (fig. S1, F and G). This increased expression in frontal lobe was already detectable in VZ and SVZ of PCW 11 neocortex by in situ hybridization (fig. S1C).

hTKTL1, not aTKTL1, increases bRG abundance

As *Tktl1* mRNA is not expressed in the embryonic mouse neocortex, this system facilitated investigation of whether ectopic expression of *hTKTL1* or *aTKTL1* would affect neuroprogenitor abundance. For this purpose, we performed in utero electroporation (IUE) of a plasmid encoding hTKTL1 or aTKTL1, or of an empty vector (control), along with a plasmid encoding green fluorescent protein (GFP) to allow the identification of the progeny of the electroporated cells, in mouse lateral neocortex at E13.5, followed by analysis at E15.5. Immunofluorescence confirmed expression of hTKTL1 and aTKTL1 in electroporated neocortex (fig. S2A).

Immunofluorescence for the mitotic markers phospho-vimentin (pVim) (Fig. 1A) and phospho-histone H3 (PH3) (fig. S2C) revealed no change in the abundance of GFP+ ventricular mitoses, which correspond to mitotic aRG, upon hTKTL1 or aTKTL1 IUE (Fig. 1B and fig. S2D). In contrast, the abundance of GFP+ mitotic BPs was increased in hTKTL1-electroporated, but not aTKTL1-electroporated, neocortex (Fig. 1C and fig. S2E). Likewise, immunofluorescence for the cycling cell marker PCNA (fig. S2F) revealed no change in the percentage of cycling APs (fig. S2G) but an increase in the percentage of cycling BPs upon hTKTL1, but not aTKTL1,

electroporation (fig. S2H). We next assessed the presence (bRG) versus absence (bIPs) of pVim+ processes among the GFP+ BPs (*12, 13*). Whereas the abundance of mitotic bIPs was not affected (Fig. 1D), the abundance of process-bearing pVim+ GFP+ BPs (i.e., bRG) was increased by a factor of 4 upon hTKTL1, but not aTKTL1, expression (Fig. 1E). Thus, mitotic bRG accounted for only ~10% of all mitotic BPs in control [as shown previously (*8–10*)] and in aTKTL1-electroporated embryonic mouse neocortex, but accounted for 33% of all mitotic BPs in hTKTL1-electroporated neocortex (fig. S2B). Hence, hTKTL1, but not aTKTL1, increases selectively bRG abundance without affecting bIP abundance.

In embryonic mouse medial neocortex, bRG abundance is greater than in lateral neocortex and is similar to that in developing gyrencephalic neocortex, with human bRG-like gene expression (*29*). Similar to embryonic mouse lateral neocortex, *hTKTL1* expression in medial neocortex increased mitotic bRG (fig. S2, I, K, and L), but not mitotic bIP (fig. S2J), abundance.

hTKTL1, not aTKTL1, increases Sox2+/Tbr2− bRG

E15.5 mouse lateral neocortex subjected to either hTKTL1, aTKTL1, or control IUE at E13.5

was analyzed by immunofluorescence for Sox2, which in the SVZ is a marker of proliferative BPs, and Tbr2, a marker of neurogenic BPs (fig. S3A). Compared to control, *hTKTL1-* and *aTKTL1-*electroporated neocortex showed no change in the percentage of GFP+ cells in the VZ that were Tbr2+ (fig. S3B), Sox2+ (fig. S3D), or Sox2+ and Tbr2− (fig. S3F). In contrast, hTKTL1, but not aTKTL1, increased the percentage of GFP+ cells in the SVZ that were Sox2+ (fig. S3E), without affecting the percentage of GFP+ cells in the SVZ that were Tbr2+ (fig. S3C). The Sox2+ BPs increased by hTKTL1 were Tbr2− (i.e., bRG) (fig. S3, G and H). We conclude that the increase in bRG abundance induced by expression of hTKTL1, but not aTKTL1, involves an increase in bRG proliferation.

bRG generate more neurons than bIPs

We considered the implications of the selective increase in bRG abundance upon hTKTL1 expression for cortical neurogenesis, based on a previous mathematical modeling of cortical neuron production by neurogenic divisions of bIPs versus bRG (*12*). In this model, as summarized in Fig. 2, A and B, both bIPs and bRG are generated by repeated asymmetric self-renewing divisions of aRG. Neuron-generating divisions of bIPs are typically symmetric consumptive, with one bIP giving rise to two neurons (Fig. 2A). In contrast, reflecting the cell polarity of bRG, in particular the presence of a basal process, neuron-generating divisions of bRG are typically asymmetric self-renewing, with one bRG producing one neuron and one bRG (Fig. 2B) (*7, 9, 10, 12, 13*). These two consecutive, asymmetric self-renewing divisions (aRG → bRG → neuron) result in an initially delayed, but eventually much more efficient, production of cortical neurons when compared to the aRG → bIP → neuron lineage (compare panels A and B of Fig. 2). We therefore modeled the consequences of the hTKTL1-induced increase in bRG abundance for cortical neuron production, assuming one round of symmetric proliferative bRG division prior to the start of the asymmetric self-renewing neuron-generating bRG divisions (Fig. 2C), as is suggested by the hTKTL1-induced increase in Sox2+ Tbr2− bRG. This resulted in an even greater increase in cortical neuron production over time (Fig. 2C). We conclude that the increase in bRG abundance by hTKTL1 but not aTKTL1 implies an increase in production of neurons over time in the developing neocortex of modern humans as compared to archaic humans.

hTKTL1 increases abundance of late-born neurons

We therefore investigated whether hTKTL1 IUE into E13.5 mouse neocortex resulted in an increase specifically in late-born neurons
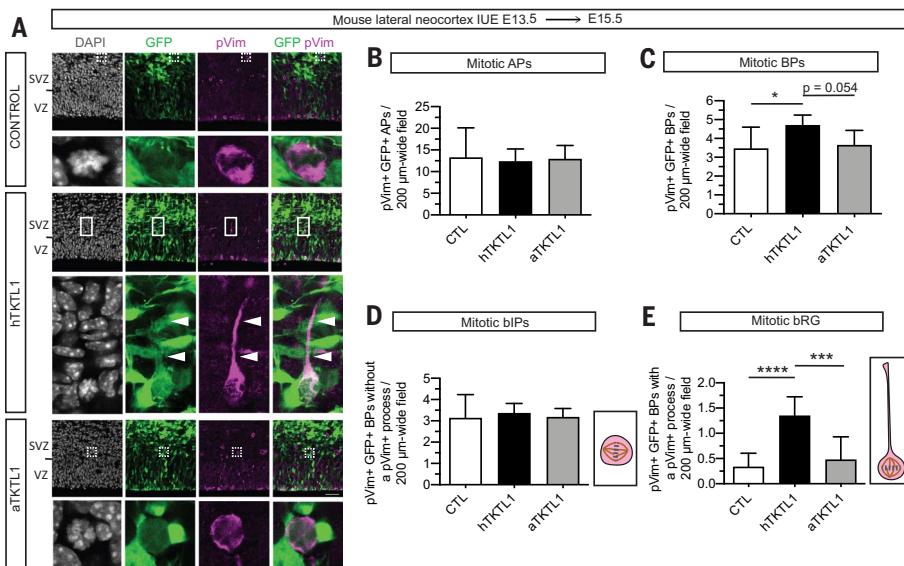
Fig. 1. Modern human TKTL1, but not archaic TKTL1, when expressed in embryonic mouse neocortex, increases mitotic bRG abundance. Mouse neocortex E13.5 IUE with GFP plasmid, together with either empty (control, CTL), hTKTL1, or aTKTL1 plasmid; analyses: E15.5. (**A**) GFP/pVim (green/magenta) immunofluorescence plus DAPI staining (gray). Bottom rows, white boxed areas at higher magnification; dashed boxed areas: GFP+/pVim+/BP without pVim+ process (mitotic bIP); solid boxed area: GFP+/pVim+/BP with pVim+ basal process (arrowheads) (mitotic bRG). Scale bar, 40 μm. (**B** to **E**) Quantifications in 200-μm-wide fields. Means of 8 embryos. Error bars, SD. (B) pVim+ GFP+ mitotic APs. One-way analysis of variance (ANOVA). (C) Total pVim+/GFP+/BPs. One-way ANOVA with Tukey post hoc test, *$P < 0.05$. (D) pVim+/GFP+/BPs without pVim+ process (mitotic bIPs). One-way ANOVA. (E) pVim+/GFP+/BPs with pVim+ process (mitotic bRG). One-way ANOVA with Tukey post hoc test, ****$P < 0.0001$, ***$P < 0.001$. Here and in the remaining figures, data reported without P values are not significant.
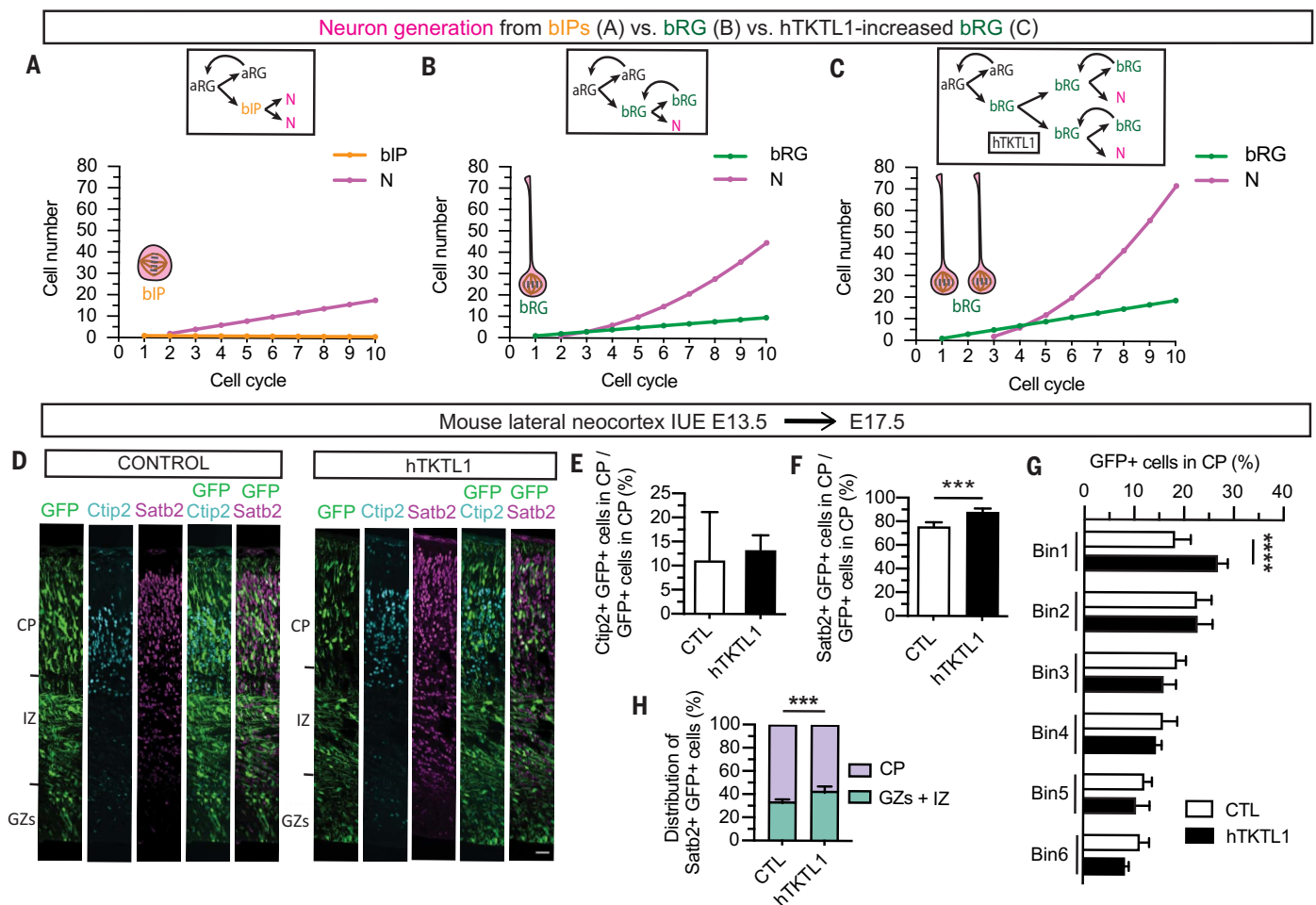
Fig. 2. The hTKTL1-induced increase in bRG in embryonic mouse neocortex results in increased production of cortical neurons, notably upper-layer neurons, at late neurogenesis. (**A** to **C**) Modeling of the number of neurons generated, over 10 cell cycles, by the aRG → bIP → neuron lineage (A), the aRG → bRG → neuron lineage (B), or the aRG → bRG → neuron lineage with one round of hTKTL1-induced symmetric proliferative bRG division (C). Curved arrows denote self-renewal. (A) and (B) are adapted from figure S4 of (*12*). (**D** to **H**) Mouse neocortex E13.5 IUE with GFP plasmid, together with either empty (control, CTL) or hTKTL1 plasmid; analyses: E17.5. (E) to (H) are means of 5 embryos. Error bars, SD. (D) GFP/Ctip2/Satb2 (green/cyan/magenta) immuno-fluorescence. Scale bar, 30 μm. [(E) and (F)] Percentages of GFP$^+$ cells in CP that are Ctip2$^+$ (E) and Satb2$^+$ (F). Unpaired Student's *t* test, (F) ***$P < 0.001$. (G) Percentages of the GFP$^+$ cells in CP that are in bins 1 to 6 (bin 1, uppermost layer; bin 6, deepest layer) of CP. Two-way ANOVA with Bonferroni post hoc test, ****$P < 0.0001$. (H) Distribution of GFP$^+$/Satb2$^+$ cells in germinal zones (GZs) plus intermediate zone (IZ) versus CP. Student's *t* test, ***$P < 0.001$.

at E17.5. To this end, we performed immuno-fluorescence for Ctip2, a marker of early-born deep-layer neurons, and for Satb2, a marker of late-born upper-layer neurons (Fig. 2D and fig. S3I). hTKTL1 expression did not affect the percentage of GFP$^+$ cells in the CP that expressed Ctip2 (Fig. 2E) but increased the percentage of GFP$^+$ cells in the CP that expressed Satb2 (Fig. 2F). Consistent with this, hTKTL1 expression increased the proportion of the GFP$^+$ cells in the CP that were located in the basal-most bin (Fig. 2G and fig. S3I). In addition, the analysis of the distribution of the Satb2$^+$ GFP$^+$ neurons across the E17.5 cortical wall revealed that in the control 66% of these neurons had reached the CP during the 4-day interval between electroporation and analysis, whereas only 57% of these neurons had reached the CP in the hTKTL1-electroporated

neocortex (Fig. 2H), as would be expected if late-born neuron generation was increased in this condition. We conclude that upon hTKTL1 expression, consistent with the mathematical modeling of the consequences of a bRG increase for cortical neuron production (Fig. 2C), the production of late-born neurons, but not that of early-born neurons, is increased.

hTKTL1 increases bRG in ferret neocortex

We investigated whether hTKTL1 expression is also able to increase bRG abundance in a gyrencephalic species, the ferret, which endogenously expresses an archaic version of TKTL1 with a lysine residue instead of the arginine residue present in hTKTL1. Similar to humans, the ferret SVZ is divided into an iSVZ and an oSVZ. We performed IUE of hTKTL1 in ferret

neocortex at E33, which corresponds to the start of the generation of the oSVZ and of the production of upper-layer neurons (*30*). This led to a factor of 4 increase in the abundance of mitotic bRG, but not mitotic bIPs, in iSVZ and oSVZ at postnatal day 2 (P2) (fig. S4, A to D). This bRG increase was accompanied by an increase in PCNA$^+$ cells (fig. S4, E and F) and Sox2$^+$/Tbr2$^-$ cells and a decrease in Tbr2$^+$ cells, in iSVZ and oSVZ (fig. S5). hTKTL1 increased the proportion of radial BPs (bRG) compared to multipolar BPs (bIPs) (fig. S4G), and within the former of bRG with multiple radial processes (*31*) at the expense of the bRG with one basal process (Fig. 3A). We conclude that ectopic expression of hTKTL1 in developing neocortex increases bRG abundance in both lissencephalic and gyrencephalic species.

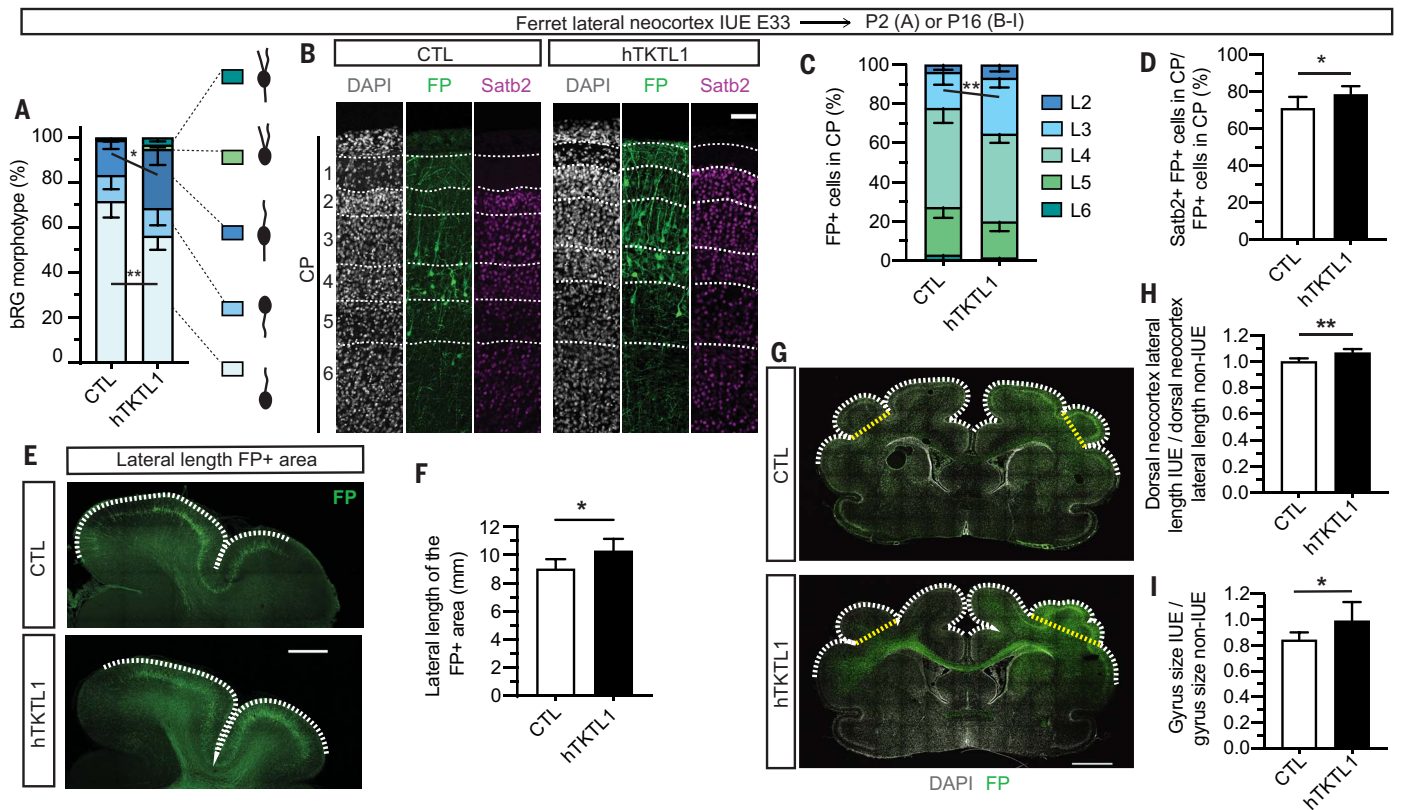Ferret lateral neocortex IUE E33 ⟶ P2 (A) or P16 (B-I)

Fig. 3. Modern human TKTL1 expressed in developing ferret neocortex increases upper-layer neuron production, neocortical surface area, and gyrus size. Ferret neocortex E33 IUE with fluorescent protein (FP) plasmid, together with either empty (control, CTL) or hTKTL1 plasmid; analyses: P2 (A) or P16 [(B) to (I)]. Means of 3 (A) or 6 [(B) to (I)] embryos. Error bars, SD. (**A**) Percentages of the 5 morphotypes of PCNA^{+} radial cells in SVZ (bRG). Two-way ANOVA with Bonferroni post hoc test, *$P < 0.05$, **$P < 0.01$. (**B**) FP/Satb2 (green/magenta) immunofluorescence plus DAPI staining (gray). White dashed lines: neuronal layers (L) 1-6 of CP. Scale bar, 75 μm. (**C**) Distribution of FP^{+} cells across L2 to L6 of the CP. Two-way ANOVA with Bonferroni post hoc test, **$P < 0.01$. (**D**) Percentage of FP^{+} cells in CP that are Satb2^{+}. Unpaired Student's t test, *$P < 0.05$. (**E**) FP (green) immunofluorescence. White dashed lines: lateral length electroporated area. Scale bar, 1 mm. (**F**) Lateral length FP[+] area. Unpaired Student's t test, *$P < 0.05$. (**G**) FP (green) immunofluorescence plus DAPI staining (gray). White dashed lines: lateral length dorsal neocortex. Yellow dashed lines: areas measured for gyrus size. Scale bar, 2 mm. (**H**) Lateral length dorsal neocortex. (**I**) Size of the gyrus showing the greatest FP immunoreactivity. [(H) and (I)] Data expressed as ratio of electroporated (IUE) over contralateral (non-IUE) hemisphere. Unpaired Student's t test, (H) **$P < 0.01$, (I) *$P < 0.05$.

hTKTL1 expands ferret upper-layer neurons and neocortex

Following IUE at E33, we analyzed ferret neocortex at P16, a developmental stage when in ferrets the cortical folds have already formed (*32, 33*). Upon hTKTL1 expression, a greater proportion of the targeted neuroprogenitor-derived progeny was now located in the upper layers of the CP, and in particular in layer 3 (Fig. 3, B and C). Corroborating this finding, hTKTL1 increased the proportion of this progeny that expressed Satb2, a transcription factor present in the majority of upper-layer neurons (Fig. 3D).

We explored whether the hTKTL1-induced increase in developing ferret neocortex in bRG abundance at P2 and upper-layer neurons at P16 affected neocortical morphology. We found (i) an increase in the lateral spread of the targeted neuroprogenitor-derived progeny at P16 (Fig. 3, E and F) and (ii) an increase in neocortical surface area as revealed by the lateral length of the dorsal neocortex (Fig. 3, G and H). Moreover, hTKTL1 expression elicited an increase in the size of the electroporated gyrus (Fig. 3, G and I). In half of the hTKTL1-electroporated neocortices (3/6), we observed a difference in the morphology of the gyral-sulcal pattern of the neocortex (fig. S6C), which, however, did not result in a significant change in the local gyrification index (fig. S6, A and B). Nonetheless, these findings demonstrate that hTKTL1 expression is sufficient to alter the morphology of a gyrencephalic neocortex.

hTKTL1 knockout reduces human bRG abundance

We examined whether, in fetal human neocortex, the endogenously expressed hTKTL1 is essential for maintaining bRG abundance. To this end, we performed a CRISPR-Cas9–mediated hTKTL1 knockout (KO) in PCW 8–14 human neocortical tissue ex vivo (see fig. S7H

for the efficiency of gRNAs). hTKTL1 KO reduced the percentage of basal GFP^{+} cells that were cycling progenitors (PCNA[+]) (Fig. 4, A and B). Immunofluorescence for HOPX [which, combined with morphological analysis, can be used to identify bRG (*20*)] revealed that hTKTL1 KO decreased the percentage of HOPX^{+} cells that have a radial morphology (i.e., bRG) among the basal GFP^{+} cells (Fig. 4, A and C). Hence, hTKTL1 is essential to maintain the full level of bRG during fetal human neocortical development.

aTKTL1-expressing organoids: Fewer bRG and neurons

We next explored the relevance for humans of our finding that hTKTL1, but not aTKTL1, increases bRG abundance. To this end, we made use of CRISPR-Cas9–mediated genome editing and "Neanderthalized" TKTL1 [by converting Arg[261] (fig. S1H) to Lys] in H9 human embryonic stem cells (ESCs). Two mock-edited
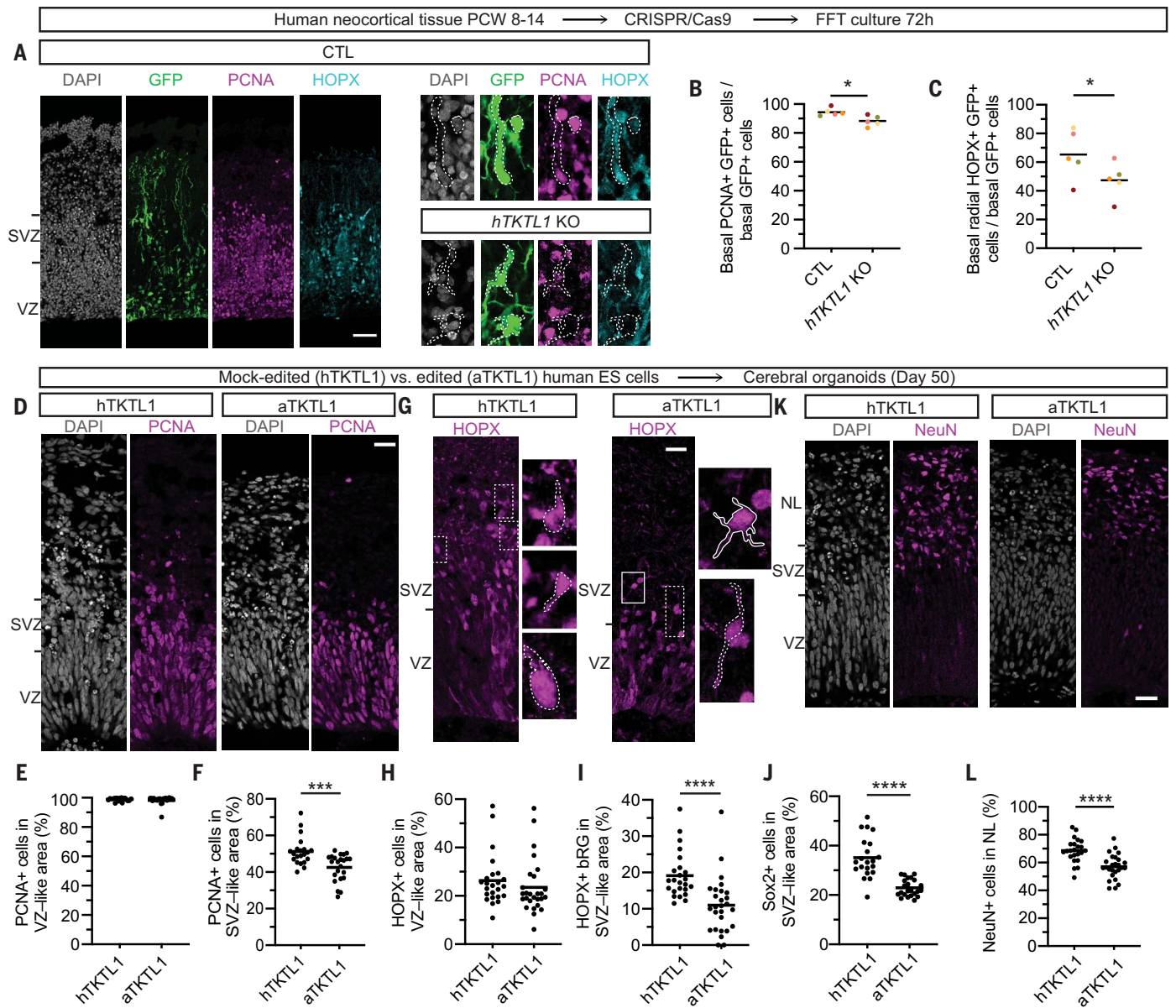
Fig. 4. *TKTL1* KO in fetal human neocortical tissue and "Neanderthalized" TKTL1 in human ESC–derived cerebral organoids reveal that modern human TKTL1 is essential to maintain the full level of bRG and neurons. (**A** to **C**) CRISPR-Cas9–mediated disruption of *hTKTL1* expression in PCW 8 to 14 fetal human neocortical tissue. Ex vivo electroporation with GFP plasmid plus complexes of recombinant Cas9 protein and gRNAs targeting *LacZ* (control, CTL) or *hTKTL1* (*hTKTL1* KO), followed by 72 hours free-floating tissue (FFT) culture. (A) GFP/PCNA/HOPX (green/magenta/cyan) immuno-fluorescence plus DAPI staining (gray). Left: CTL electroporation. Right: abventricular cells for CTL (top) and *hTKTL1* KO (bottom). White dashed lines: cell morphology. CTL: GFP⁺/PCNA⁺/HOPX⁺ radial cell (bRG), GFP⁺/PCNA⁺/ weakly HOPX⁺ cell (multipolar in different optical section, bIP). *hTKTL1*-KO: multipolar GFP⁺/PCNA⁺/HOPX⁻ cell (bIP, top cell), multipolar GFP⁺/PCNA⁻/ HOPX⁻ cell (neuron, bottom cell). Scale bar, 50 μm. [(B) and (C)] Percentages of basal GFP⁺ cells that are PCNA⁺ (B) and HOPX⁺ with radial morphology (C). Means of 5 different fetal samples. Paired Student's *t* test, *P < 0.05. (**D** to **L**) Human embryonic stem cells (ESCs, H9 line) were CRISPR-Cas9– mediated genome-edited to convert *hTKTL1* (Arg) to *aTKTL1* (Lys). Organoids grown from two mock-edited (hTKTL1-1, hTKTL1-2) and two edited (aTKTL1-1, aTKTL1-2) lines; analyses: day 50. (D) PCNA (magenta) immunofluorescence plus DAPI-staining (gray). Scale bar, 25 μm. [(E) and (F)] Percentages of PCNA⁺ cells in VZ-like (E) and SVZ-like (F) areas. Means of 21 hTKTL1 (9 hTKTL1-1, 12 hTKTL1-2) and 23 aTKTL1 (12 aTKTL1-1, 11 aTKTL1-2) organoids. Mann-Whitney U test, ***P < 0.001. (G) HOPX (magenta) immunofluorescence. Right sides: white boxes at higher magnification; dashed lines: radial cells; solid line: multipolar cell. Scale bar, 25 μm. [(H) and (I)] Percentages of HOPX⁺ cells in VZ-like area (H) and HOPX⁺ radial cells in SVZ-like area (I). Means of 24 hTKTL1 (11 hTKTL1-1, 13 hTKTL1-2) and 27 aTKTL1 (19 aTKTL1-1, 8 aTKTL1-2) organoids. Mann-Whitney U test, (I) ****P < 0.0001. (J) Percentages of Sox2⁺ cells in the VZ-like area. Means of 21 hTKTL1 (9 hTKTL1-1, 12 hTKTL1-2) and 23 aTKTL1 (12 aTKTL1-1, 11 aTKTL1-2) organoids. Mann-Whitney U test, ****P < 0.0001. (K) NeuN (magenta) immunofluorescence plus DAPI-staining (gray). Scale bar, 25 μm. (L) Percentage of NeuN⁺ cells in neuronal layer (NL). Means of 23 hTKTL1 (9 hTKTL1-1, 14 hTKTL1-2) and 26 aTKTL1 (12 aTKTL1-1, 14 aTKTL1-2) organoids. Unpaired Student's *t* test, ****P < 0.0001.

hTKTL1 (Arg) and two edited *aTKTL1* (Lys) H9 lines were generated, all of which (i) expressed established markers of pluripotency (fig. S7, A and B); (ii) did not show any chromosomal aneuploidies and large-scale chromosomal duplications and deletions in comparison to the mother H9 ESC line used for genome editing, as revealed by shallow DNA sequencing (fig. S7C); and (iii) showed identical karyograms (fig. S7D). The two mock-edited and the two *aTKTL1*-edited H9 lines were used to generate cerebral organoids (fig. S8A) that were analyzed at day 50. In situ hybridization showed that *TKTL1* mRNA is expressed in the germinal zones of the cerebral organoids (fig. S8B).

The percentage of cycling cells (PCNA$^+$) in the VZ-like area did not differ between the hTKTL1-expressing and aTKTL1-expressing organoids (Fig. 4, D and E). However, the percentage of cycling cells in the SVZ-like area was reduced in the aTKTL1-expressing organoids (Fig. 4, D and F). Moreover, aTKTL1-expressing organoids showed no change in the percentage of HOPX$^+$ cells (Fig. 4, G and H) or of Sox2$^+$ cells (fig. S8, C and D) in the VZ-like area, but a decrease in the percentage of HOPX$^+$ cells with a radial morphology (bRG) (Fig. 4, G and I) and of Sox2$^+$ cells (Fig. 4J and fig. S8C) in the SVZ-like area. Consistent with the reduction in bRG, the *TKTL1*-"Neanderthalized" cerebral organoids exhibited a reduction in the percentage of cells in the layer (referred to as neuronal layer) that express the neuronal markers NeuN (Fig. 4, K and L) and Hu (fig. S8, E and F). The reduction in bRG and neurons observed in aTKTL1-expressing organoids was not due to an increase in cell death (fig. S8G). Taken together, these data show that the Arg^{261} in hTKTL1 is essential for the generation of the full level of bRG and neurons in human cerebral organoids.

Pentose phosphate pathway inhibition abolishes hTKTL1-induced bRG increase

We sought to obtain insight into the mechanism of action of hTKTL1. TKTL1 belongs to the transketolase family (*18*), and TKT, the founding member of this family, is known to operate in the pentose phosphate pathway (PPP), an action also reported for TKTL1 (*18*, *19*) (Fig. 5A). Thus, TKTL1 has been reported to cleave xylulose 5-phosphate, a metabolite in the PPP, into glyceraldehyde 3-phosphate and acetate (*19*) (Fig. 5A). We therefore examined a possible role of the PPP in the hTKTL1-induced increase in bRG abundance. We used 6-aminonicotinamide (6-AN), an NADP analog, to inhibit 6-phosphogluconate dehydrogenase (6PGDH), the enzyme converting 6-phosphogluconate into ribulose 5-phosphate in the PPP (Fig. 5A). 6-AN is 400 times more potent to inhibit 6PGDH than to inhibit other

NADP-dependent enzymes (*34*). E13.5 mouse neocortex was electroporated with a plasmid encoding hTKTL1 or an empty vector, along with a plasmid encoding GFP. The brain was dissected 24 hours after IUE and subjected to HERO culture for 24 hours in the absence or presence of 6-AN (fig. S9A). 6-AN at 50 and 100 μM completely suppressed the hTKTL1-induced increase in mitotic bRG (Fig. 5C and fig. S9, B and C) without significantly affecting the essentially equal levels upon control versus hTKTL1 IUE of mitotic bIPs (Fig. 5B) and mitotic aRG (fig. S9D). The lack of effect on bIP and aRG numbers by 6-AN treatment implies that this drug, even at 100 μM, did not exert unspecific effects on neuroprogenitors. Consistent with these data for mitotic neuroprogenitors, treatment with 50 μM or 100 μM 6-AN completely suppressed the hTKTL1-induced increase in the percentage of GFP$^+$ cells in the SVZ that were Sox2$^+$ (fig. S9, E and G) but had no effect on the percentage of these cells in the VZ (fig. S9F), nor did it affect the percentage of GFP$^+$ cells in the SVZ that were Sox2$^+$ upon control IUE (fig. S9G).

To corroborate these results, we inhibited 6PGDH with a different pharmacological inhibitor, 1-hydroxy-8-methoxyanthracene-9,10-dione (S3). Using the same experimental model, we found that the hTKTL1-induced increase in mitotic bRG was partially reduced upon treatment with 10 μM S3 and abolished upon treatment with 20 μM S3 (fig. S10, A and D). This treatment had no effect on mitotic aRG (fig. S10B) and mitotic bIP abundance (fig. S10C). Accordingly, treatment with 10 or 20 μM S3 suppressed the hTKTL1-induced increase in the percentage of GFP$^+$ cells in the SVZ that are Sox2$^+$ (fig. S10, E and G) without affecting the percentage of these cells in the VZ (fig. S10F). Taken together, these results demonstrate that the hTKTL1-induced increase in bRG abundance requires the PPP, specifically the 6-phosphogluconate to ribulose 5-phosphate conversion (see Fig. 5A).

PPP inhibition reduces human neocortical bRG

To examine the physiological relevance of these data, we subjected PCW 11–13 human neocortical tissue, which endogenously expresses *hTKTL1*, to free-floating tissue (FFT) culture for 2 days in the presence or absence of the PPP inhibitors 6-AN or S3. Treatment with 50 or 100 μM 6-AN reduced the abundance of mitotic bRG by ~60% (Fig. 5, D and F) but did not affect the abundance of mitotic bIPs (Fig. 5, D and E). Likewise, treatment with 5, 10, or 20 μM S3 reduced the abundance of mitotic bRG by ~40 to 55% (fig. S10, H and J) but did not affect the abundance of mitotic bIPs (fig. S10I). The reductions in bRG observed upon 6-AN and S3 treatments were not due to an increase in apoptosis (fig. S9, H and I, and fig. S10, K and L). We conclude that the

6-phosphogluconate to ribulose 5-phosphate conversion step in the PPP, which is required for the hTKTL1-induced increase in bRG abundance in embryonic mouse neocortex (Fig. 5C; fig. S9, C and G; and fig. S10, D and G), is also required for the maintenance of the physiological bRG level in fetal human neocortex, indicating a role of the PPP in this maintenance.

Fatty acid synthesis inhibition abolishes hTKTL1-induced bRG increase

One of the metabolites generated by the reactions in the PPP downstream of the 6-phosphogluconate to ribulose 5-phosphate conversion step is glyceraldehyde 3-phosphate, which via conversion to pyruvate in the glycolysis pathway can eventually give rise to acetyl–coenzyme A (CoA) (Fig. 5A). In addition, TKTL1 has been reported to cleave xylulose 5-phosphate, a metabolite in the PPP, into glyceraldehyde 3-phosphate and acetate. The latter, too, can be further processed to acetyl-CoA (*19*) (Fig. 6A). As it has been reported that TKTL1—via elevated acetyl-CoA levels—promotes fatty acid synthesis (*19*), we explored whether increased fatty acid synthesis is involved in the hTKTL1-induced increase in bRG abundance. Fatty acid synthesis starts with the conversion of acetyl-CoA to malonyl-CoA by the enzyme acetyl-CoA carboxylase (ACACA) (Fig. 6A). We therefore subjected mouse neocortex, hTKTL1- and control-electroporated at E13.5, to HERO culture starting at E14.5 in the absence or presence of 5-(tetradecyloxy)-2-furoic acid (TOFA), an inhibitor of ACACA. Analysis after 24 hours of HERO culture revealed that the hTKTL1-induced increase in mitotic bRG was halved upon treatment with 10 μM, and abolished with 20 or 50 μM, TOFA (Fig. 6C and fig. S11, A and C). TOFA treatment did not affect the equal levels upon control versus hTKTL1 IUE of mitotic APs (fig. S11B) or mitotic bIPs (Fig. 6B). Consistent with these data for mitotic neuroprogenitors, TOFA treatment suppressed the hTKTL1-induced increase in the percentage of GFP$^+$ cells in the SVZ that were Sox2$^+$ (fig. S11, D and F) but had no effect on the percentage of these cells in the VZ (fig. S11E), nor did it affect the percentage of GFP$^+$ cells in the SVZ that were Sox2$^+$ upon control IUE (fig. S11F).

These results were corroborated using a second inhibitor of ACACA, ND-646. Treatment with 5 μM ND-646, using the same experimental model, abolished the hTKTL1-induced increase in the percentage of GFP$^+$ cells in the SVZ that were Sox2$^+$ (fig. S12, A and C) without affecting these cells in the VZ (fig. S12B). These results demonstrate that the hTKTL1-induced increase in bRG abundance requires the conversion of acetyl-CoA in malonyl-CoA.

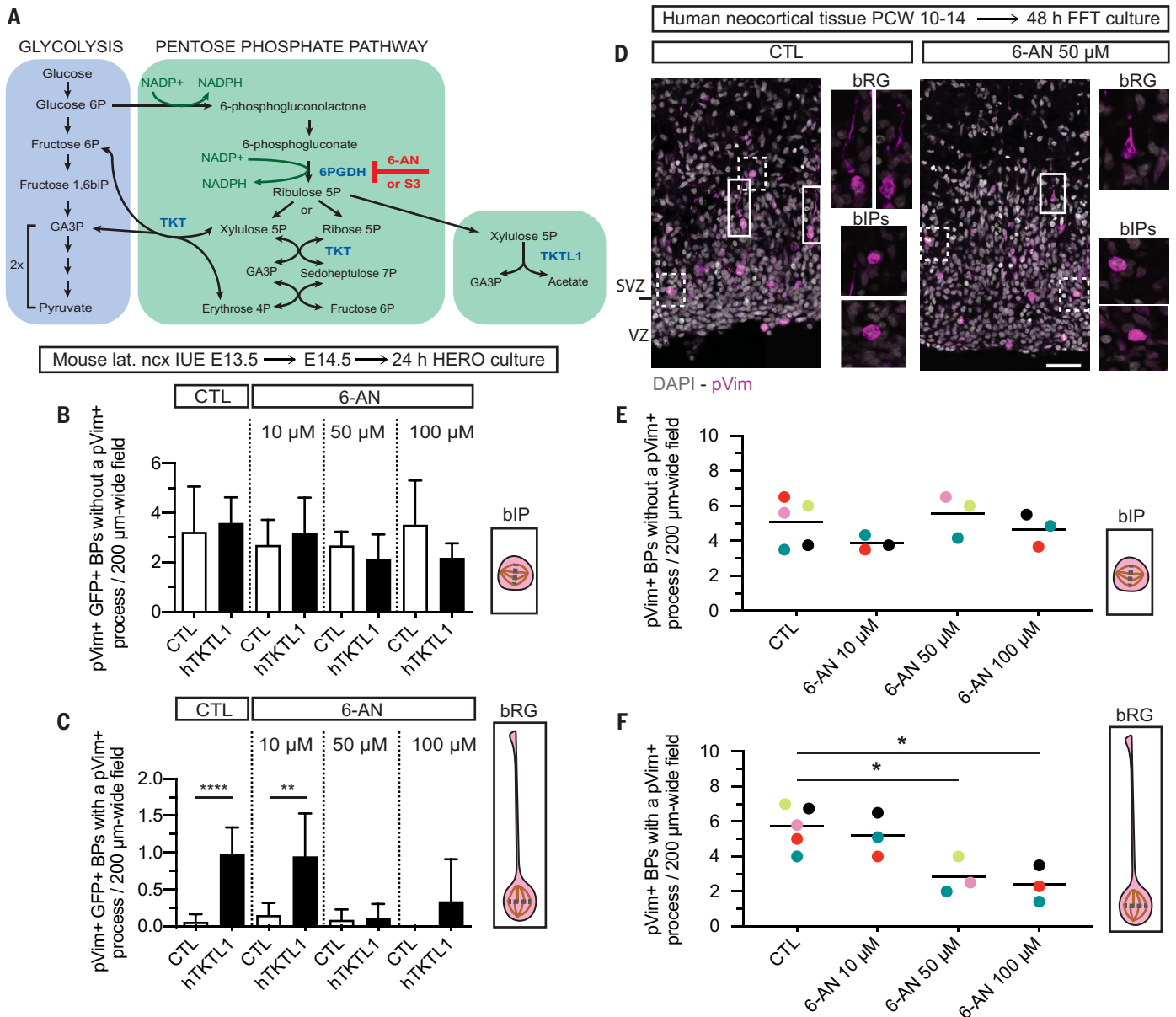To further analyze the requirement of fatty acid synthesis in the hTKTL1-induced increase

Fig. 5. Inhibition of the pentose phosphate pathway abolishes the hTKTL1-induced increase in bRG in embryonic mouse neocortex and reduces bRG abundance in fetal human neocortex. (**A**) Schematic representation of the glycolysis and pentose phosphate pathways. Known TKT, and proposed TKTL1 (*19*), sites of action are indicated. 6-Aminonicotinamide (6-AN) and S3: 6-phosphogluconate dehydrogenase (6PGDH) inhibitors. (**B** and **C**) Mouse lateral neocortex (lat. ncx.) E13.5 IUE with GFP plasmid, together with empty (control, CTL) or hTKTL1 plasmid. E14.5: Hemisphere rotation culture (HERO, 24 hours) in the absence or presence of 10, 50, or 100 μM 6-AN. Quantifications of pVim$^+$/GFP$^+$/BPs without pVim$^+$ process (mitotic bIPs) (B) and with pVim$^+$ process (mitotic bRG) (C) in 200-μm-wide fields. Means of 3 to 9 embryos. Error bars, SD. (B) Two-way ANOVA; (C) two-way ANOVA with Bonferroni post hoc test, ****$P < 0.0001$, **$P < 0.01$. (**D** to **F**) Free-floating tissue culture (FFT, 48 hours) of human neocortical tissue (PCW 10 to 14) for 48 hours, without or with 10, 50, or 100 μM 6-AN. (D) pVim (magenta) immunofluorescence plus DAPI staining (gray). Right sides: white boxed areas at higher magnification; pVim$^+$/BP without pVim$^+$ process (mitotic bIP, dashed lines), and with pVim$^+$ process (mitotic bRG, solid lines). Scale bar, 40 μm. [(E) and (F)] Quantification of pVim$^+$/BPs without pVim$^+$ process (mitotic bIPs) (E) and with pVim$^+$ process (mitotic bRG) (F) in 200-μm-wide field. Means of 3 to 5 fetal samples, each a different color. (E) One-way ANOVA; (F) one-way ANOVA with Tukey post hoc test, *$P < 0.05$.

in bRG abundance, we explored whether the following step of fatty acid synthesis, the condensation of acetyl-CoA and malonyl-CoA by fatty acid synthase (FAS), is required. Using our standard approach of hTKTL1 IUE at E13.5, E14.5 neocortex was subjected to HERO culture for 24 hours in the absence or presence of the FAS inhibitor Orlistat. Orlistat at 10 and 20 μM completely suppressed the hTKTL1-induced increase in mitotic bRG (fig. S13, A and D) without affecting mitotic bIPs (fig. S13C) and mitotic aRG (fig. S13B). Accordingly, treatment with 10 μM or 20 μM Orlistat completely suppressed the hTKTL1-induced increase in the percentage of GFP$^+$ cells in the SVZ that were Sox2$^+$ (fig. S13, E and G) without affecting these cells in the VZ (fig. S13F). These data therefore demonstrate that hTKTL1 induced the increase in bRG abundance through a fatty acid synthesis–dependent mechanism.
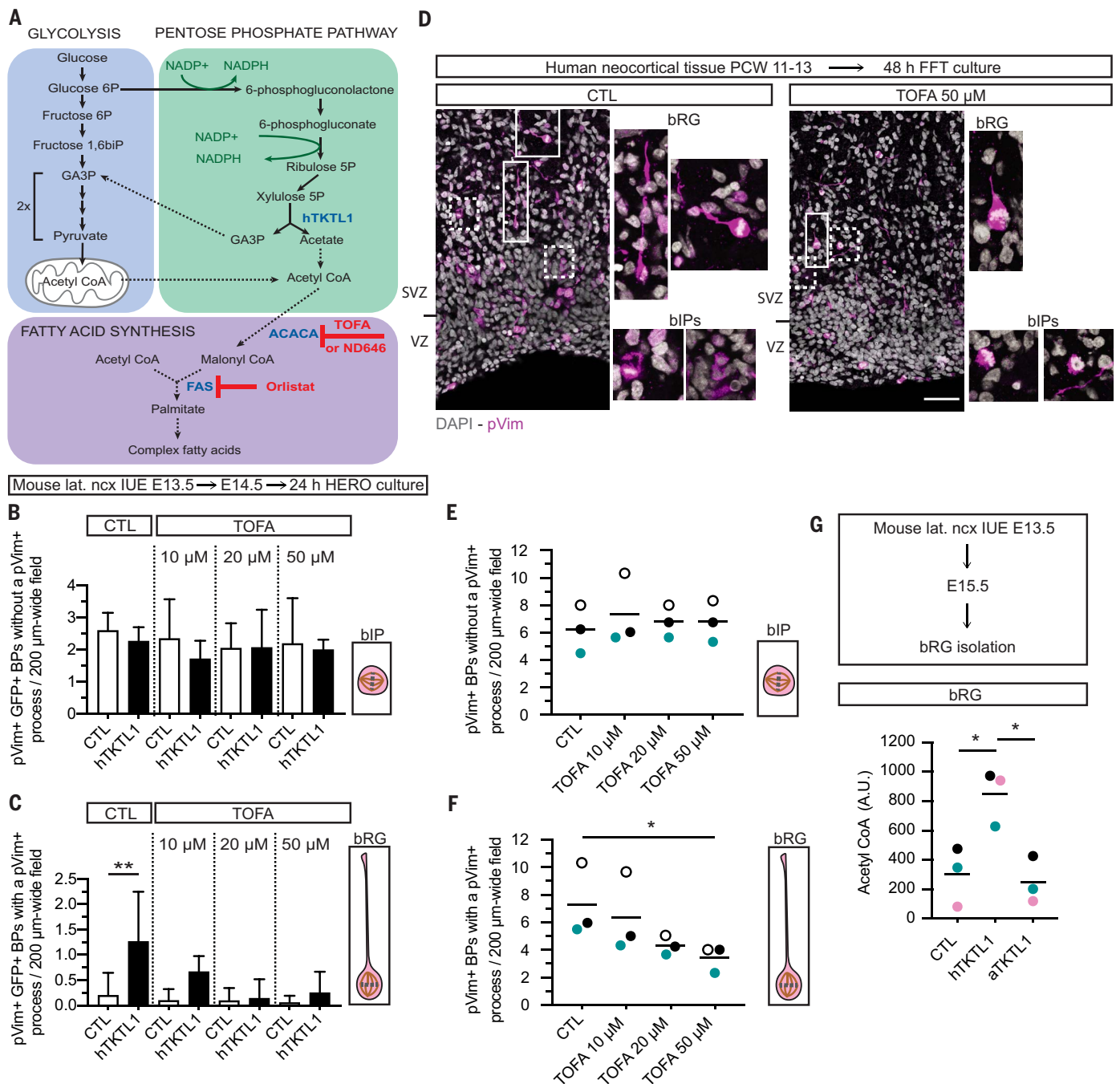
Fig. 6. Inhibition of fatty acid synthesis abolishes the hTKTL1-induced increase in bRG in embryonic mouse neocortex and reduces bRG abundance in fetal human neocortex. (**A**) Schematic representation of the glycolysis, pentose phosphate, and fatty acid synthesis pathways. Proposed TKTL1 site of action (*19*) indicated. 5-(Tetradecyloxy)-2-furoic acid (TOFA) and ND646: acetyl-CoA carboxylase (ACACA, conversion of acetyl-CoA into malonyl-CoA, fatty acid synthesis first and rate-limiting step) inhibitors. Orlistat: fatty acid synthase (FAS) inhibitor. (**B** and **C**) Mouse lateral neocortex E13.5 IUE with GFP plasmid, together with either an empty (control, CTL) or an hTKTL1 plasmid. E14.5: Hemisphere rotation culture (HERO, 24 hours), in the absence or presence of 10, 20, or 50 µM TOFA. Quantification of pVim⁺/GFP⁺/BPs without pVim⁺ process (mitotic bIPs) (B) and with pVim⁺ process (mitotic bRG) (C) in 200-µm-wide field. Means of 5 to 7 embryos. Error bars, SD. (B) Two-way ANOVA; (C) two-way ANOVA with Bonferroni post hoc test, **P < 0.01. (**D** to **F**) Free-floating tissue culture (FFT, 48 hours) of human neocortical tissue (PCW 11 to 13), without or with 10, 20, or 50 µM TOFA. (D) pVim (magenta) immunofluorescence plus DAPI staining (gray). Right side: white boxed areas at higher magnification; pVim⁺/BP without pVim⁺ process (mitotic bIP, dashed lines), and with pVim⁺ process (mitotic bRG, solid lines). Scale bar, 50 µm. [(E) and (F)] Quantification of pVim⁺/BPs without pVim⁺ process (mitotic bIPs) (E) and with pVim⁺ process (mitotic bRG) (F) in 200-µm-wide field. Means of 3 fetal samples, each a different color. (E) One-way ANOVA; (F) Friedman test with Dunn post hoc test, *P < 0.05. (**G**) Mouse lateral neocortex E13.5 IUE with GFP plasmid, together with either empty (control, CTL), hTKTL1, or aTKTL1 plasmid. E15.5 GFP⁺/bRG isolation by FACS. Acetyl-CoA concentration in arbitrary units (A.U., see methods). Means of 3 bRG isolations, each a different color. One-way ANOVA with Tukey post hoc test, *P < 0.05.

We also used our mouse test system (neocortex hTKTL1 IUE → HERO culture) to explore potentially additive effects when inhibitors of both the PPP and fatty acid synthesis are used together. 6-AN at 10 μM [which, in light of its affinity for 6PGDH, is likely to partially inhibit the PPP (*34*)] plus 10 μM TOFA partially reduced the hTKTL1-induced increase in the level of bRG (fig. S11, G and J) to a similar extent as 10 μM TOFA alone (Fig. 6C). 6-AN at 50 μM plus 20 μM TOFA completely abolished the hTKTL1-induced increase in the level of bRG (fig. S11J) similarly to 6-AN (Fig. 5C) and TOFA (Fig. 6C) alone. Neither treatment with both inhibitors together affected mitotic bIPs (fig. S11I) and mitotic aRG (fig. S11H). On the likely assumption that partial inhibition of the PPP still provides sufficient acetyl-CoA levels for fatty acid synthesis to occur, the lack of an additive effect of 10 μM 6-AN plus 10 μM TOFA on bRG reduction is consistent with the model (Fig. 6A) that fatty acid synthesis is rate-limiting for the generation of bRG and that the pentose phosphate pathway is upstream of fatty acid synthesis by providing acetyl-CoA.

Fatty acid synthesis inhibition reduces human neocortical bRG

To examine the physiological relevance of these data, we asked whether inhibition of fatty acid synthesis in fetal human neocortex, which endogenously expresses *hTKTL1*, would reduce bRG abundance. To this end, we treated fetal human neocortical tissue in FFT culture for 48 hours with 10, 20, or 50 μM TOFA. Treatment with 50 μM TOFA decreased the abundance of mitotic bRG, identified as process-bearing pVim⁺ BPs (Fig. 6, D and F), but not that of mitotic bIPs, identified as process-lacking pVim⁺ BPs (Fig. 6, D and E). Furthermore, human neocortical tissue treated for 48 hours with either (i) 5 μM ND-646 or (ii) 10 or 20 μM Orlistat reduced the abundance of mitotic bRG (fig. S12, D and F, and fig. S13, H and J), but not of mitotic bIPs (fig. S12, D and E, and fig. S13, H and I). The reductions in bRG observed upon TOFA, ND646, and Orlistat treatments were not due to an increase in apoptosis (fig. S11, K and L; fig. S12, G and H; and fig. S13, K and L). Hence, fatty acid synthesis, which is required for the hTKTL1-induced increase in bRG abundance in embryonic mouse neocortex (Fig. 6C and fig. S13D), is also required to maintain the abundance of bRG in fetal human neocortex.

hTKTL1 increases acetyl-CoA concentration in bRG

Our data with the various inhibitors of the PPP and fatty acid synthesis suggest a mechanism in which the increase in bRG abundance by hTKTL1 involves an increase in fatty acid synthesis, which is enabled by hTKTL1's action in the PPP that increases the relevant precur-

sor metabolites for fatty acid synthesis. If so, one would expect an increase in the concentration of acetyl-CoA in bRG upon hTKTL1 expression. We therefore used mass spectrometry to determine the acetyl-CoA concentration in bRG isolated from E15.5 control-, hTKTL1- and aTKTL1-electroporated mouse neocortex (IUE at E13.5). This showed that, indeed, the acetyl-CoA concentration was higher in bRG isolated from hTKTL1-electroporated neocortex than in bRG isolated from control-electroporated neocortex (Fig. 6G). The ability of TKTL1 to increase acetyl-CoA concentration in bRG is restricted to hTKTL1, as bRG isolated from aTKTL1-electroporated neocortex had a similar concentration in acetyl-CoA as the control (Fig. 6G).

Discussion

Our results provide insight into the development of the neocortex of modern humans compared to that of archaic humans. This insight is based on the present findings pertaining to *TKTL1*, a gene belonging to the transketolase family that arose in mammals and that, reflecting its involvement in various types of human cancer, has been implicated in cell proliferation.

hTKTL1 affects bRG, not other neuroprogenitors

The human-specific variant *hTKTL1* increases the abundance, among the various types of neuroprogenitors, of bRG. Upon overexpression in embryonic mouse neocortex, hTKTL1 was found in all types of neuroprogenitors. The selective action of hTKTL1, but not aTKTL1, on bRG abundance has physiological relevance, as KO of *hTKTL1* alone was sufficient to reduce the normal bRG level in fetal human neocortical tissue. The selectivity of hTKTL1 for bRG is likely related to the need of bRG for de novo membrane biogenesis in order to proliferate.

Single amino acid substitution underlies hTKTL1 effect

Previous studies reported on the role of single modern human-specific amino acid substitutions in adenylosuccinate lyase, an enzyme involved in purine metabolism (*35*), and in NOVA1, a splicing regulator involved in neuronal maturation (*36*) [but see (*37*)]. Our results identify the functional role of a single modern human-specific amino acid substitution in the control of the abundance of one type of neuroprogenitor during neocortex development. The lysine-to-arginine substitution that occurred during human evolution (*27*) allows hTKTL1 to ensure the elevated bRG numbers characteristic of fetal human neocortex. Not only the reduction in bRG numbers upon *hTKTL1* KO in fetal human neocortical tissue, but also the lower bRG numbers in cerebral organoids expressing archaic TKTL1,

support this conclusion. Our data therefore imply a difference in cortical neuroprogenitor composition between Neanderthals and modern humans.

hTKTL1 action requires the PPP

Our demonstration that the ability of hTKTL1 to ensure elevated bRG numbers requires the PPP adds another case to the emerging concept of a role of metabolism in neuroprogenitor proliferation (*38*) and of human-specific molecular changes affecting this metabolism. Another example is the human-specific gene *ARHGAP11B*, the protein of which acts in mitochondria and promotes BP proliferation by stimulating glutaminolysis (*39*). This ability of ARHGAP11B is based on a single C → G nucleotide substitution (*40*). The ability of hTKTL1 to ensure elevated bRG numbers via its action in the PPP is also based on a single A → G nucleotide substitution that converts the lysine in archaic TKTL1 into the arginine of modern human TKTL1.

Our data show that bRG numbers, in contrast to bIP numbers, depend on the PPP. Given the inability of aTKTL1 to increase bRG abundance, it is worth considering how the single amino acid substitution (lysine to arginine) in TKTL1 during human evolution may have affected its metabolic function. The side chain of arginine is a much stronger base than that of lysine, which may be advantageous for the enzymatic reaction reported for hTKTL1, that is, to cleave xylulose 5-phosphate into glyceraldehyde 3-phosphate and acetate (*19*).

hTKTL1 action requires fatty acid synthesis

The ability of hTKTL1 to ensure elevated bRG numbers via fatty acid synthesis is in agreement with a previous finding that knockdown of *hTKTL1* in the THP-1 leukemia cell line, which expresses high levels of *hTKTL1* mRNA, led to the reduction of the amount of several lipids containing fatty acids (*19*), and with the notion that fatty acid synthesis is a feature of highly proliferative cells, such as cancer cells (*41*). In this context, the role of the essential precursor to fatty acid synthesis, acetyl-CoA, in hTKTL1 action is further supported by our demonstration that hTKTL1, but not aTKTL1, increases acetyl-CoA levels in bRG.

To understand how fatty acid synthesis might be related to bRG proliferation, one should consider that fatty acids are building blocks for membrane synthesis and that the number of bRG cell processes has been shown to be linked to bRG proliferative capacity (*31*). bRG with an increased number of cell processes have been proposed to be able to sense additional extrinsic signals, which in turn activate pro-proliferative signaling pathways. Hence, hTKTL1 is likely to stimulate bRG proliferation, and hence bRG abundance, by promoting cell process growth via synthesis of fatty

acids that are then used to build membranes. In support of this notion, hTKTL1 expression in developing ferret neocortex increased the proportion of bRG with multiple radial processes.

hTKTL1 may influence neocortex shape

Our findings that hTKTL1 expression in developing ferret neocortex increases its lateral extension and gyrus size raise the possibility that hTKTL1 played a role in determining the shape of the neocortex of modern humans. Endocast analyses indicate that Neanderthals and modern humans had/have a similar endocranial volume, consistent with similar brain size (*5*), but that the shape of their brains was/is different. The skull of modern humans has a globular shape, whereas the skull of Neanderthals had a more elongated shape, which is typical of the living apes (*5*). In this context, hTKTL1 could be involved in the formation of a more globular neocortex in modern humans. In addition, modern humans have a larger parietotemporal lobe than Neanderthals (*42*). In support of a possible role of hTKTL1 in neocortical regionalization, it has been reported that *hTKTL1* mRNA expression in PCW 15–21 fetal human neocortex is enriched in the oSVZ of the frontal, as compared to caudal, neocortex (*28*). Consistent with these data, we found an increase in *hTKTL1* mRNA levels in the human frontal lobe compared to the occipital lobe. Hence, hTKTL1 could have played a role in the expansion of the frontal lobe of the neocortex of modern humans.

Neurogenesis in modern humans versus Neanderthals

An implication of the ability of hTKTL1 to ensure elevated bRG numbers pertains to a difference in cortical neuron production between modern humans and Neanderthals. As is evident from our mathematical modeling (Fig. 3, A to C), cortical neuron production over time is greater with bRG than bIPs. In line with this, we observed an increase specifically in late-born (i.e., upper-layer) neurons upon hTKTL1 expression. As such an increase is a hallmark of neocortex development during human evolution (*6*), the selective increase in bRG numbers upon hTKTL1, but not aTKTL1, expression implies that during human evolution, modern humans acquired a more efficient mode of cortical neuron production than Neanderthals. Consistent with this notion, human cerebral organoids expressing archaic TKTL1 showed not only a reduction in bRG, but also in neurons.

The higher *TKTL1* mRNA expression in the frontal lobe than in other parts of the fetal human neocortex suggests that the increase in cortical neuron production pertains, in particular, to the frontal lobe of the neocortex of modern humans. Furthermore, the increase in cortical neuron production, resulting from the elevated bRG numbers due to hTKTL1 action, presumably contributes to the fact that modern humans generate the largest number of cortical neurons of all living primates (*43*).

Conclusions

Our study demonstrates that the gene *hTKTL1* of modern humans is sufficient to increase the abundance of bRG, a neuroprogenitor type that has a role in neocortical evolution. This increase in bRG abundance is induced by the modern human variant of TKTL1 and not by its archaic variant. This suggests that a single human-specific amino acid substitution in TKTL1 underlies changes in cell metabolism that ultimately result in a specific composition of neuroprogenitors and features of cortical neurogenesis that distinguish modern humans from Neanderthals and other extinct archaic humans.

Methods summary

IUE of embryonic mouse neocortex

IUE was performed as described (*31*). E13.5 (for lateral neocortex) or E15.5 (for medial neocortex) embryos were injected intraventricularly with a solution containing 0.1% Fast Green (Sigma) in PBS, 1 μg/μl of pCAGGS plasmid (either empty vector, hTKTL1, or aTKTL1) and 0.4 μg/μl or 1 μg/μl (for cell sorting) of pCAGGS-GFP. The embryos were then electroporated and sacrificed at E15.5 or E17.5 (for lateral neocortex) or at E18.5 (for medial neocortex).

IUE of embryonic ferret neocortex

E33 ferret neocortex was electroporated as described (*44*). The embryos were injected intraventricularly with 0.1% Fast Green (Sigma) in PBS, 2.5 μg/μl of either empty pCAGGS (control) or pCAGGS-hTKTL1, and 1 μg/μl of either pCAGGS-GFP or pCAGGS-mCherry. The injected embryos were electroporated. After birth, the pups were sacrificed at P2 or P16.

Mouse cerebral hemisphere rotation culture

Cerebral hemispheres were dissected from E14.5 mouse embryos 24 hours after IUE at E13.5, and the electroporated hemispheres were placed into hemisphere rotation (HERO) culture as described (*45*), with minor modifications. Hemispheres were cultured with mouse slice culture medium containing 0.1% DMSO and either no addition (control) or one of the inhibitors, for 24 hours at 37°C, in a whole-embryo culture incubator (Ikemoto Scientific Technology).

Human neocortex free-floating tissue culture

Free-floating tissue (FFT) culture of fetal human neocortex (PCW 8–14) was performed for 48 hours (inhibitors) or 72 hours (CRISPR/Cas9 KO) as described (*46*). For the pharmacological inhibitor studies, the tissue was incubated with 0.1% DMSO and either no further addition (control) or one of the inhibitors. The flasks were incubated for 48 or 72 hours at 37°C in a whole-embryo culture incubator (Ikemoto Scientific Technology).

Human fetal neocortical tissue electroporation

Ex vivo electroporation of human fetal neocortical tissue was performed as described (*39*). Human fetal neocortical tissue was electroporated using a mixture of either the Cas9–LacZ-gRNA complex (control) or the Cas9–hTKTL1-gRNA complex, Fast Green, pCAGGS-GFP, and glycerol, followed by 72-hour FFT culture.

Cerebral organoids

Two mock-edited (hTKTL1) and two gene-edited (aTKTL1) H9 cell lines were differentiated into cerebral organoids using previously published protocols (*47*, *48*). The cerebral organoids were fixed at day 50 with PFA at 4°C for 2 hours.

Cryosectioning and immunofluorescence

Cryosectioning of fixed tissues (including cerebral organoids) was performed as described (*31*). Immunofluorescence of cryosections subjected to antigen retrieval was performed as described (*29*).

bRG isolation and determination of acetyl-CoA

We used a modification of a published procedure (*22*) to isolate bRG from E15.5 mouse neocortices, identified as GLAST-positive and prominin-1–negative cells, after IUE at E13.5 (GFP plus either empty vector, hTKTL1, or aTKTL1). bRG were isolated from the neocortical cell suspension by FACS. Acetyl-CoA levels in the FACS-isolated bRG were determined by mass spectrometry.

Other methods

All other methods used were carried out according to standard procedures.

REFERENCES AND NOTES

1. M. Breyl, Triangulating Neanderthal cognition: A tale of not seeing the forest for the trees. *Wiley Interdiscip. Rev. Cogn. Sci.* **12**, e1545 (2021). doi: 10.1002/wcs.1545; pmid: 32918796
2. D. L. Hoffmann *et al.*, U-Th dating of carbonate crusts reveals Neandertal origin of Iberian cave art. *Science* **359**, 912–915 (2018). doi: 10.1126/science.aap7778; pmid: 29472483
3. D. Leder *et al.*, A 51,000-year-old engraved bone reveals Neanderthals' capacity for symbolic behaviour. *Nat. Ecol. Evol.* **5**, 1273–1282 (2021). doi: 10.1038/s41559-021-01487-z; pmid: 34226702
4. P. Rakic, Evolution of the neocortex: A perspective from developmental biology. *Nat. Rev. Neurosci.* **10**, 724–735 (2009). doi: 10.1038/nrn2719; pmid: 19763105
5. P. Gunz *et al.*, Neandertal introgression sheds light on modern human endocranial globularity. *Curr. Biol.* **29**, 120–127.e5 (2019). doi: 10.1016/j.cub.2018.10.065; pmid: 30554901
6. J. H. Lui, D. V. Hansen, A. R. Kriegstein, Development and evolution of the human neocortex. *Cell* **146**, 18–36 (2011). doi: 10.1016/j.cell.2011.06.030; pmid: 21729779
7. E. Taverna, M. Götz, W. B. Huttner, The cell biology of neurogenesis: Toward an understanding of the development and evolution of the neocortex. *Annu. Rev. Cell Dev. Biol.* **30**,

465–502 (2014). doi: 10.1146/annurev-cellbio-101011-155801; pmid: 25000993

8. I. Kelava et al., Abundant occurrence of basal radial glia in the subventricular zone of embryonic neocortex of a lissencephalic primate, the common marmoset Callithrix jacchus. Cereb. Cortex 22, 469–481 (2012). doi: 10.1093/cercor/bhr301; pmid: 22114084

9. X. Wang, J. W. Tsai, B. LaMonica, A. R. Kriegstein, A new subtype of progenitor cell in the mouse embryonic neocortex. Nat. Neurosci. 14, 555–561 (2011). doi: 10.1038/nn.2807; pmid: 21478886

10. A. Shitamukai, D. Konno, F. Matsuzaki, Oblique radial glial divisions in the developing mouse neocortex induce self-renewing progenitors outside the germinal zone that resemble primate outer subventricular zone progenitors. J. Neurosci. 31, 3683–3695 (2011). doi: 10.1523/JNEUROSCI.4773-10.2011; pmid: 21389223

11. M. Betizeau et al., Precursor diversity and complexity of lineage relationships in the outer subventricular zone of the primate. Neuron 80, 442–457 (2013). doi: 10.1016/j.neuron.2013.09.032; pmid: 24139044

12. S. A. Fietz et al., OSVZ progenitors of human and ferret neocortex are epithelial-like and expand by integrin signaling. Nat. Neurosci. 13, 690–699 (2010). doi: 10.1038/nn.2553; pmid: 20436478

13. D. V. Hansen, J. H. Lui, P. R. Parker, A. R. Kriegstein, Neurogenic radial glia in the outer subventricular zone of human neocortex. Nature 464, 554–561 (2010). doi: 10.1038/nature08845; pmid: 20154730

14. V. Borrell, M. Götz, Role of radial glial cells in cerebral cortex folding. Curr. Opin. Neurobiol. 27, 39–46 (2014). doi: 10.1016/j.conb.2014.02.007; pmid: 24632307

15. A. Pinson, W. B. Huttner, Neocortex expansion in development and evolution—from genes to progenitor cell biology. Curr. Opin. Cell Biol. 73, 9–18 (2021). doi: 10.1016/j.ceb.2021.04.008; pmid: 34098196

16. J. F. Coy et al., Molecular cloning of tissue-specific transcripts of a transketolase-related gene: Implications for the evolution of new vertebrate genes. Genomics 32, 309–316 (1996). doi: 10.1006/geno.1996.0124; pmid: 8838793

17. B. L. Horecker, The pentose phosphate pathway. J. Biol. Chem. 277, 47965–47971 (2002). doi: 10.1074/jbc.X200002700; pmid: 12403765

18. J. F. Coy, D. Dressler, J. Wilde, P. Schubert, Mutations in the transketolase-like gene TKTL1: Clinical implications for neurodegenerative diseases, diabetes and cancer. Clin. Lab. 51, 257–273 (2005). pmid: 15991799

19. S. Diaz-Moralli et al., A key role for transketolase-like 1 in tumor metabolic reprogramming. Oncotarget 7, 51875–51897 (2016). doi: 10.18632/oncotarget.10429; pmid: 27391434

20. A. A. Pollen et al., Molecular identity of human outer radial glia during cortical development. Cell 163, 55–67 (2015). doi: 10.1016/j.cell.2015.09.004; pmid: 26406371

21. S. A. Fietz et al., Transcriptomes of germinal zones of human and mouse fetal neocortex suggest a role of extracellular matrix in progenitor self-renewal. Proc. Natl. Acad. Sci. U.S.A. 109, 11836–11841 (2012). doi: 10.1073/pnas.1209647109; pmid: 22753484

22. M. Florio et al., Human-specific gene ARHGAP11B promotes basal progenitor amplification and neocortex expansion. Science 347, 1465–1470 (2015). doi: 10.1126/science.aaa1975; pmid: 25721503

23. M. B. Johnson et al., Single-cell analysis reveals transcriptional heterogeneity of neural progenitors in human cortex. Nat. Neurosci. 18, 637–646 (2015). doi: 10.1038/nn.3980; pmid: 25734491

24. W. Sun et al., TKTL1 is activated by promoter hypomethylation and contributes to head and neck squamous cell carcinoma carcinogenesis through increased aerobic glycolysis and HIF1α

stabilization. Clin. Cancer Res. 16, 857–866 (2010). doi: 10.1158/1078-0432.CCR-09-2604; pmid: 20103683

25. R. Peltonen et al., High TKTL1 expression as a sign of poor prognosis in colorectal cancer with synchronous rather than metachronous liver metastases. Cancer Biol. Ther. 21, 826–831 (2020). doi: 10.1080/15384047.2020.1803008; pmid: 32795237

26. W. Yuan et al., Silencing of TKTL1 by siRNA inhibits proliferation of human gastric cancer cells in vitro and in vivo. Cancer Biol. Ther. 9, 710–716 (2010). doi: 10.4161/cbt.9.9.11431; pmid: 20200485

27. K. Prüfer et al., The complete genome sequence of a Neanderthal from the Altai Mountains. Nature 505, 43–49 (2014). doi: 10.1038/nature12886; pmid: 24352235

28. J. A. Miller et al., Transcriptional landscape of the prenatal human brain. Nature 508, 199–206 (2014). doi: 10.1038/nature13185; pmid: 24695229

29. S. Vaid et al., A novel population of Hopx-dependent basal radial glial cells in the developing mouse neocortex. Development 145, dev169276 (2018). doi: 10.1242/dev.169276; pmid: 30266827

30. M. A. Martínez-Martínez et al., A restricted period for formation of outer subventricular zone defined by Cdh1 and Trnp1 levels. Nat. Commun. 7, 11812 (2016). doi: 10.1038/ncomms11812; pmid: 27264089

31. N. Kalebic et al., Neocortical expansion due to increased proliferation of basal progenitors is linked to changes in their morphology. Cell Stem Cell 24, 535–550.e9 (2019). doi: 10.1016/j.stem.2019.02.017; pmid: 30905618

32. N. Matsumoto, Y. Shinmyo, Y. Ichikawa, H. Kawasaki, Gyrification of the cerebral cortex requires FGF signaling in the mammalian brain. eLife 6, e29285 (2017). doi: 10.7554/eLife.29285; pmid: 29132503

33. V. Fernández, C. Llinares-Benadero, V. Borrell, Cerebral cortex expansion and folding: What have we learned? EMBO J. 35, 1021–1044 (2016). doi: 10.15252/embj.201593701; pmid: 27056680

34. J. S. Hothersall, M. Gordge, A. A. Noronha-Dutra, Inhibition of NADPH supply by 6-aminonicotinamide: Effect on glutathione, nitric oxide and superoxide in J774 cells. FEBS Lett. 434, 97–100 (1998). doi: 10.1016/S0014-5793(98)00959-4; pmid: 9738459

35. V. Stepanova et al., Reduced purine biosynthesis in humans after their divergence from Neandertals. eLife 10, e58741 (2021). doi: 10.7554/eLife.58741; pmid: 33942714

36. C. A. Trujillo et al., Reintroduction of the archaic variant of NOVA1 in cortical organoids alters neurodevelopment. Science 371, eaax2537 (2021). doi: 10.1126/science.aax2537; pmid: 33574182

37. T. Maricic et al., Comment on "Reintroduction of the archaic variant of NOVA1 in cortical organoids alters neurodevelopment". Science 374, eabi6060 (2021). doi: 10.1126/science.abi6060; pmid: 34648345

38. T. Namba, J. Nardelli, P. Gressens, W. B. Huttner, Metabolic regulation of neocortical expansion in development and evolution. Neuron 109, 408–419 (2021). doi: 10.1016/j.neuron.2020.11.014; pmid: 33306962

39. T. Namba et al., Human-specific ARHGAP11B acts in mitochondria to expand neocortical progenitors by glutaminolysis. Neuron 105, 867–881.e9 (2020). doi: 10.1016/j.neuron.2019.11.027; pmid: 31883789

40. M. Florio, T. Namba, S. Pääbo, M. Hiller, W. B. Huttner, A single splice site mutation in human-specific ARHGAP11B causes basal progenitor amplification. Sci. Adv. 2, e1601941 (2016). doi: 10.1126/sciadv.1601941; pmid: 27957544

41. F. Röhrig, A. Schulze, The multifaceted roles of fatty acid synthesis in cancer. Nat. Rev. Cancer 16, 732–749 (2016). doi: 10.1038/nrc.2016.89; pmid: 27658529

42. M. Bastir, A. Rosas, D. E. Lieberman, P. O'Higgins, Middle cranial fossa anatomy and the origin of modern humans. Anat.

Rec. 291, 130–140 (2008). doi: 10.1002/ar.20636; pmid: 18213701

43. S. Herculano-Houzel, The remarkable, yet not extraordinary, human brain as a scaled-up primate brain and its associated cost. Proc. Natl. Acad. Sci. U.S.A. 109 (suppl. 1), 10661–10668 (2012). doi: 10.1073/pnas.1201895109; pmid: 22723358

44. N. Kalebic et al., Human-specific ARHGAP11B induces hallmarks of neocortical expansion in developing ferret neocortex. eLife 7, e41241 (2018). doi: 10.7554/eLife.41241; pmid: 30484771

45. J. Schenk, M. Wilsch-Bräuninger, F. Calegari, W. B. Huttner, Myosin II is required for interkinetic nuclear migration of neural progenitors. Proc. Natl. Acad. Sci. U.S.A. 106, 16487–16492 (2009). doi: 10.1073/pnas.0908928106; pmid: 19805325

46. K. R. Long et al., Extracellular matrix components HAPLN1, lumican, and collagen I cause hyaluronic acid-dependent folding of the developing human neocortex. Neuron 99, 702–719.e6 (2018). doi: 10.1016/j.neuron.2018.07.013; pmid: 30078576

47. M. A. Lancaster, J. A. Knoblich, Generation of cerebral organoids from human pluripotent stem cells. Nat. Protoc. 9, 2329–2340 (2014). doi: 10.1038/nprot.2014.158; pmid: 25188634

48. F. Mora-Bermúdez et al., Differences and similarities between human and chimpanzee neural progenitors during cerebral cortex development. eLife 5, e18683 (2016). doi: 10.7554/eLife.18683; pmid: 27669147

ACKNOWLEDGMENTS

SUPPLEMENTARY MATERIALS

Science

Human TKTL1 implies greater neurogenesis in frontal neocortex of modern humans than Neanderthals

Anneline PinsonLei XingTakashi NambaNereo KalebicJula PetersChristina Eugster OegemaSofia TraikovKatrin ReppeStephan RiesenbergTomislav MaricicRazvan DerihaciPauline WimbergerSvante PääboWieland B. Huttner

Neanderthal brain development

Neanderthal brains were similar in size to those of modern humans but differed in shape. What we cannot tell from fossils is how Neanderthal brains might have differed in function or organization of brain layers such as the neocortex. Pinson *et al.* have now analyzed the effect of a single amino acid change in the transketolase-like 1 (TKTL1) protein on production of basal radial glia, the workhorses that generate much of the neocortex (see the Perspective by Malgrange and Nguyen). Modern humans differ from apes and Neanderthals by this single amino acid change. When placed in organoids or overexpressed in nonhuman brains, the human variant of TKTL1 drove more generation of neuroprogenitors than did the archaic variant. The authors suggest that the modern human has more neocortex to work with than the ancient Neanderthal did. —PJH

View the article online
https://www.science.org/doi/10.1126/science.abl6422
Permissions
https://www.science.org/help/reprints-and-permissions

Use of this article is subject to the Terms of service